SPECTRAL ANALYSIS WINDOWING

A window is the aperture through which we examine the world. By necessity, any time or spatial signal we observe, collect, and process must have bounded support. Similarly any time or spatial signal we approximate, design, and synthesize must also have bounded support. Bounded support is the range or width of the independent variable (time, distance, or frequency) over which the dependent variable, say the signal, is nonzero. This finite support can be defined over multiple dimensions, for instance, extending over a line, a plane, or a volume. Windows can be continuous functions or discrete sequences defined over their appropriate finite supports.

At the simplest level, a window can be considered a multiplicative operator that turns on the signal within the finite support and turns it off outside that same support. This operator affects the signal's Fourier transform in a number of undesired ways; the most significant is by undesired out-of-band side-lobe levels. The size and order of the discontinuities exhibited by the signal governs the level and rate of attenuation of these spectral side-lobes. Other unwanted effects include spectral smearing and in-band ripple. The design and application of windows is directed to minimizing or controlling the undesired artifacts of in-band ripple, out-of-band side-lobes, and spectral smearing.

Examples of the application of windows to control finite aperture effects can be found in numerous disciplines. These include the following:

1. *Finite Duration Filter Impulse Response (FIR) Design.* Windows applied to a prototype filter's impulse response to control transition bandwidth and levels of in-band and out-of-band side-lobes.
2. *Spectrum Analysis, Transforms of Sliding, Overlapped, Windowed Data.* Windows applied to observed time series to control variance of spectral estimate while suppressing spectral leakage (additive bias).
3. *Power Spectra as Transform of Windowed Correlation Functions.* Windows applied to a sample correlation function to suppress segments of the sample correlation function exhibiting high bias and variance.
4. *Nonstationary Spectra and Model Estimates.* Windows applied to delayed and overlapped collection time series to localize time and spectral features (model parameters) of nonstationary signals.
5. *Modulation Spectral Mask Control.* Design of modulation envelope to control spectral side-lobe behavior.
6. *Synthetic Aperture RADAR (SAR).* Windows applied to spatial series to control antenna side-lobes.
7. *Phased Array Antenna Shading Function.* Window applied to spatial function to control antenna side-lobes.
8. *Photolithography Apodizing Function.* Smooth transmission function applied to optical aperture to control diffraction pattern side-lobes.

We will discuss a subset of these applications later in this chapter. For convenience and consistency, we will consider the window as being applied to a time domain signal. The window can, of course, be applied to any function with the same intent and goal. The common theme of these applications is control of envelope smoothness in the time domain to obtain desired properties in the frequency domain.

WINDOWS IN SPECTRUM ANALYSIS

A concept we now take for granted is that a signal can be described in different coordinate systems and that there is engineering value in examining a signal described in an alternate basis system. One basis system we find particularly useful is the set of complex exponentials. The attraction of this basis set is that complex exponentials are the eigen-functions and eigen-series of linear time invariant (LTI) differential and difference operators, respectively. Put in its simplest form, this means that when a sinewave is applied to an LTI filter the steady-state system response is a scaled version of the same sinewave. The system can only affect the complex amplitude (magnitude and phase) of the sinewave but can never change its frequency. Consequently complex sinusoids have become a standard tool to probe and describe LTI systems. The process of describing a signal as a summation of scaled sinusoids is standard Fourier transform analysis. The Fourier transform and Fourier series, shown in Eq. (1), permits us to describe signals equally well in both the time domain and the frequency domain:

$$\begin{aligned} H(\omega) &= \int_{-\infty}^{+\infty} h(t)e^{-j\omega t}\,dt, \\ H(\theta) &= \sum_{-\infty}^{+\infty} h(n)e^{-j\theta n} \\ h(t) &= \frac{1}{2\pi}\int_{-\infty}^{+\infty} H(\omega)e^{+j\omega t}d\,\omega, \\ h(n) &= \frac{1}{2\pi}\int_{-\pi}^{+\pi} H(\theta)e^{+j\theta n}\,d\theta \end{aligned} \tag{1}$$

Since the complex exponentials have infinite support, the limits of integration in the forward transform (time-to-frequency) are from minus to plus infinity. As observed earlier, all signals of engineering interest have finite support, which motivates us to modify the limits of integration of the Fourier transform to reflect this restriction. This is shown in Eq. (2) where T_{SUP} and N define the finite supports of the signal.

$$\begin{aligned} H_{\text{SUP}}(\omega) &= \int_{T_{\text{SUP}}} h(t)e^{-j\omega t}\,dt, \\ H_{\text{SUP}}(\theta) &= \sum_{N} h(n)e^{-j\theta n} \\ h(t) &= \frac{1}{2\pi}\int_{-\infty}^{+\infty} H_{\text{SUP}}(\omega)e^{+j\omega t}\,d\omega, \\ h(n) &= \int_{-\pi}^{+\pi} H_{\text{SUP}}(\theta)e^{-j\theta n}\,d\theta \end{aligned} \tag{2}$$

The two versions of the transform can be merged in a single compact form if we use a finite support window to limit the signal to the appropriate finite support interval, as opposed to using the limits of integration or limits of summation. This is shown as

$$\begin{aligned} H_{\text{SUP}}(\omega) = H_W(\omega) &= \int_{-\infty}^{+\infty} w(t)\cdot h(t)e^{-j\omega t}\,dt, \\ H_{\text{SUP}}(\theta) = H_W(\theta) &= \sum_{-\infty}^{+\infty} w(n)\cdot h(n)e^{-j\theta n} \\ h(t) &= \frac{1}{2\pi}\int_{-\infty}^{+\infty} H_W(\omega)e^{+j\omega t}\,d\omega, \\ h(n) &= \frac{1}{2\pi}\int_{-\pi}^{+\pi} H_W(\theta)e^{+j\theta n}\,d\theta \end{aligned} \tag{3}$$

A natural question to ask when examining Eq. (3) is how has limiting the signal extent with the multiplicative window affected the transform of the signal? The simple answer is related to the relationship that multiplication of two functions (or sequences) in the time (or sequence) domain is equivalent to convolution of their spectra in the frequency domain. As shown in Eq. (4), the transform of the windowed signal is the convolution of the transform of the signal with the transform of the window:

$$\begin{aligned} H_W(\omega) &= \frac{1}{2\pi}\int_{-\infty}^{+\infty} H(\lambda)\cdot W(\omega-\lambda)\,d\lambda, \\ H_W(\theta) &= \frac{1}{2\pi}\int_{-\pi}^{+\pi} H(\lambda)\cdot W(\theta-\lambda)\,d\lambda \\ H(\omega) &= \frac{1}{2\pi}\int_{-\infty}^{+\infty} h(t)e^{-j\omega t}\,d\omega, \\ H(\theta) &= \sum_{-\infty}^{+\infty} h(n)e^{-j\theta n} \\ W(\omega) &= \frac{1}{2\pi}\int_{-T/2}^{+T/2} w(t)e^{-j\omega t}\,d\omega, \\ W(\theta) &= \sum_{-N/2}^{+N/2} w(n)e^{-j\theta n} \end{aligned} \tag{4}$$

This relationship and its impact on spectral analysis can be dramatically illustrated by examining the Fourier transform of a single sinusoid on an infinite support and on a finite support. Figure 1 shows the time and frequency representation of the rectangle window, of a sinusoid of infinite duration, and of a finite support sinusoid obtained as a product of the previous two signals. Eqs. (5a) and (5b) describe the same signals and their corresponding transforms:

$$\begin{aligned} w(t) &= \begin{cases} 1 & -\frac{T}{2} < t < \frac{T}{2} \\ 0 & \text{otherwise} \end{cases} \\ W(f) &= T\frac{\sin(\pi fT)}{(\pi fT)} \\ s(t) &= A\,\sin(2\pi f_0 t-\phi),\ \infty < t < +\infty \\ S(f) &= \frac{A}{2}e^{-j\varphi}\,\delta(f-f_0)+\frac{A}{2}e^{+j\varphi}\,\delta(f+f_0) \\ s_W(t) &= A\,\sin(2\pi f_0 t-\phi),\ -\frac{T}{2} < t < +\frac{T}{2} \\ S_W(f) &= \frac{AT}{2}e^{-j\varphi}\frac{\sin[\pi(f-f_0)T]}{[\pi(f-f_0)T]}+\frac{AT}{2}e^{+j\varphi}\frac{\sin[\pi(f+f_0)T]}{[\pi(f+f_0)T]} \end{aligned} \tag{5a}$$

$$\begin{aligned} w(n) &= \begin{cases} 1 & -\frac{N}{2} < n < \frac{N}{2} \\ 0 & \text{otherwise} \end{cases} \\ W(\theta) &= \frac{\sin(\theta N/2)}{\sin(\theta/2)} \\ s(n) &= A\,\sin(\theta_0 n-\phi),\ \infty < n < +\infty \\ S(\theta) &= \frac{A}{2}e^{-j\varphi}\,\delta(\theta-\theta_0)+\frac{A}{2}e^{+j\varphi}\,\delta(\theta+\theta_0) \\ s_W(n) &= A\,\sin(\theta_0 n-\phi),\ -\frac{N}{2} < n < +\frac{N}{2} \\ S_W(\theta) &= \frac{A}{2}e^{-j\varphi}\frac{\sin[(\theta-\theta_0)N/2]}{\sin[(\theta-\theta_0)/2]}+\frac{A}{2}e^{+j\varphi}\frac{\sin[(\theta+\theta_0)N/2]}{\sin[(\theta+\theta_0)/2]} \end{aligned} \tag{5b}$$

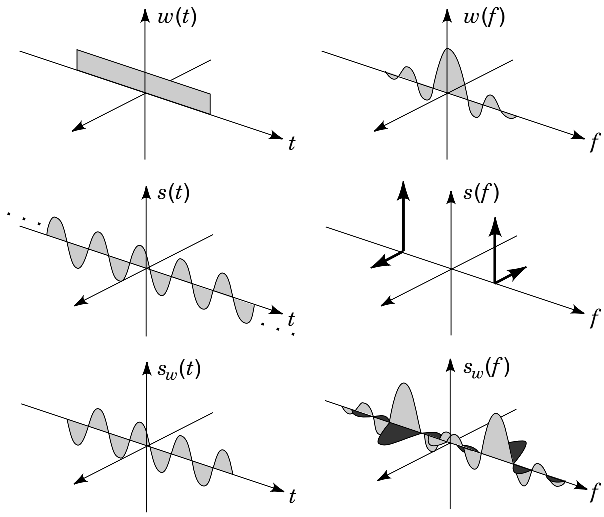

Figure 1. Time and spectral description of rectangle window, sinusoid, and windowed sinusoid.

As we can see, the transform of the windowed sinusoid, being the convolution of a pair of spectral impulses located at $f = \pm f_0$ with $\sin(\pi fT)/(\pi fT)$ or $\text{sinc}(\pi fT)$ which is the transform of the window, results in the window's transform being scaled and translated to the frequency of the impulses. This can be considered as a special case of the modulation theorem shown in Eq. (6) where we can consider the time function $h(t)$ to be the window $w(t)$:

Modulation Theorem

If $h(t)$ has a transform $H(f)$,

$$\text{then } h(t)\, e^{j2\pi f_0 t} \text{ has a transform } H(f - f_0). \tag{6}$$

The effects of the window on the spectrum of a signal can be readily seen in Fig. 1. Here we note that the Fourier transform of the constant envelope sinusoid has zero width. The first effect we observe is a smearing of the transforms spectral width (from infinitesimally small to the main lobe of the $\sin(\pi fT)/(\pi fT)$). The second effect is spectral leakage, the spreading of the singularity to the $\sin(\pi fT)/(\pi fT)$ side-lobes, a function occupying an infinite support with an envelope exhibiting a spectral decay rate of $1/f$.

The side-lobe structure of the windowed transform limits the ability of the transform to detect spectral components of significantly smaller amplitude in the presence of a large-amplitude component, while the main-lobe width of the windowed transform limits the ability of the transform to resolve or separate nearby spectral components. The first of these limitations is demonstrated in Fig. 2 where a stylized power spectrum of two sinusoids of infinite extent and of finite extent is presented. For this example the relative amplitude of the low-level signal at frequency f_2 is 60 dB below the high-level signal at f_1. Note that the side-lobe structure of the high-level signal is greater than the main-lobe level of the low-level signal; hence it masks the presence of the low-level signal. If the low-level signal is to be detected in the presence of the nearby high-level signal, the window applied to the data must be modified. Windows must be selected with side-lobe structure significantly lower than the side-lobe structure of the rectangle window.

A comment is called for on this example. Under the restricted condition that the frequencies of the two signals are harmonically related to the observation interval (i.e., that the two signals each exhibit an integer number of cycles in the observation interval), the two signals would be resolvable and measurable. The reason is that for the conditions described, the two signals are orthogonal. When interpreted in the frequency domain, this means that the spectrum of the second signal is located on a zero crossing of the spectrum of the first signal. We will discuss this special condition and similar examples in the section on windows and the discrete Fourier transform (DFT).

As mentioned earlier, the main-lobe width of the windowed transform limits the ability of the transform to resolve closely spaced spectral components of comparable amplitudes. This limitation is demonstrated in Fig. 3, where we demonstrate loss of resolvability of two signals as the spectra of two sinusoids of finite support are brought closer together.

In this example the amplitude of the two signals is the same, and the interaction between the phase of the main-lobes and the interaction between the main-lobes and the neighbor's side-lobes has been ignored. It is apparent that the spacing between adjacent spectral lines that can be resolved by a windowed transform is related to the main-lobe width of the window's spectrum. For the rectangle window, this main-lobe width (measured from peak to first zero crossing) is $1/T$, the reciprocal of the window's duration in the time domain. We will find in the next section that as we modify windows to obtain a desired reduction in side-lobe levels, this side-lobe reduction is accompanied by an increase in main-lobe width,

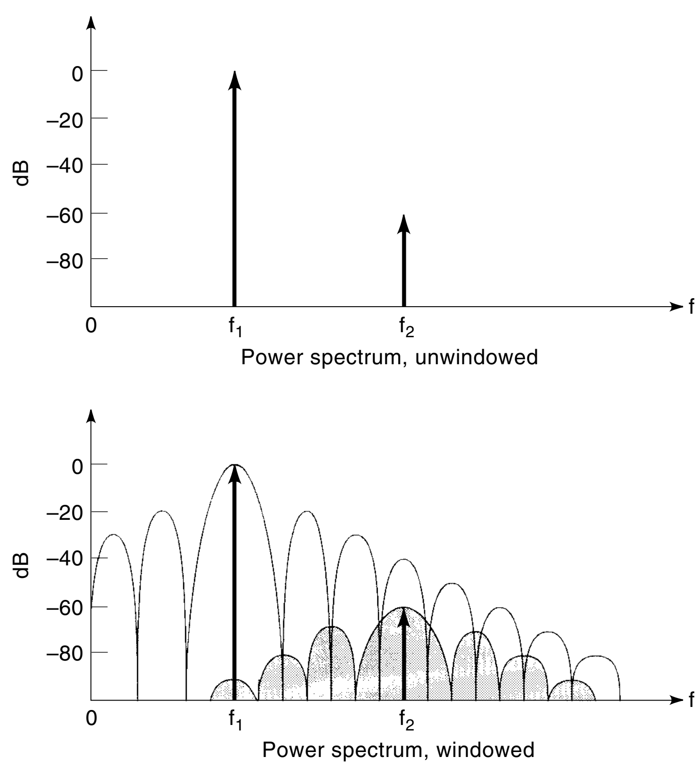

Figure 2. Spectral representation of unwindowed and of a rectangle windowed sinusoids of significantly different amplitudes.

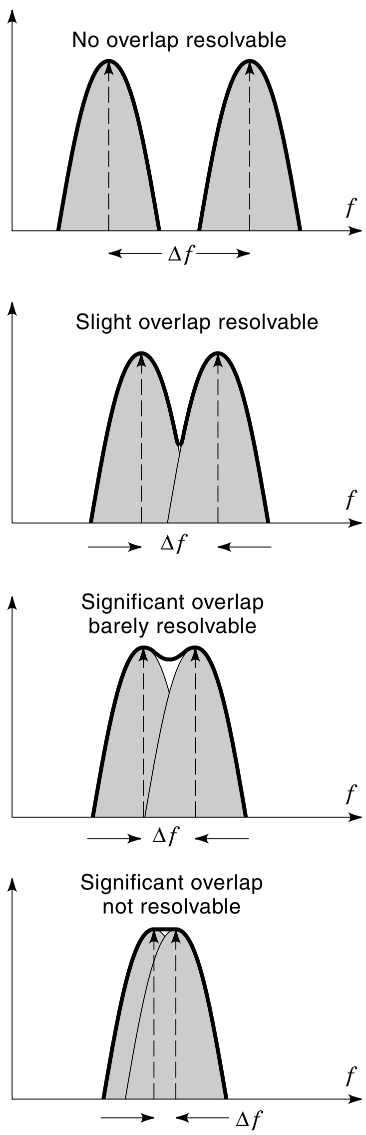

Figure 3. Spectral representation of windowed sinusoids of successively decreasing spectral distance demonstrating loss of resolution due to merging of main-lobe responses.

which reduces the spectral resolution capabilities of the window.

WINDOWS AS A SUM OF COSINES

We cannot build windows without side-lobes in their spectra. What we can do is design windows with arbitrarily low-level side-lobes. We can accomplish this with a number of design tools, which we will examine shortly. The common mechanism of these tools is that they control side-lobe levels by controlling the smoothness of the window in the time domain. We will demonstrate how the window smoothness in the time domain and window side-lobe levels in the frequency domain is coupled. Figure 4 presents the time and spectral description of the rectangle window. We note the spectrum is the ubiquitous $\sin(\pi fT)/(\pi fT)$ or $\text{sinc}(\pi fT)$. This represents a spectrum centered at zero frequency with main-lobe width $1/T$ and with amplitude of its first spectral side-lobe of $2/3\pi$, or -13.5 dB below the main-lobe peak. The way to reduce the side-lobes is to destructively cancel them by the side-lobes of judicially placed pairs of scaled $\text{sinc}(\pi(f \pm f_0)T)$ functions. One popular option is to translate a pair of $\text{sinc}(\pi fT)$ functions to the first zero crossings of the $\text{sinc}(\pi fT)$ function. These zeros are located at frequency $\pm 1/T$, the first frequency orthogonal to the rectangle window of length T. These $\text{sinc}(\pi fT)$ functions represent a cosine with period exactly equal to the support of the rectangle window (frequency $= 1/T$). As seen in the figure, the side-lobes contributed by the additional pair present opposing polarity side-lobes to those of the original $\text{sinc}(\pi fT)$ function. The effect of adding three $\text{sinc}(\pi fT)$ functions is now obvious: The main-lobe width is doubled, and the side-lobe levels are reduced by an amount dependent on the particular values of a_k.

The window just constructed is called a raised cosine window and is a member of a class of windows formed by a short cosine Fourier transform of the form

$$
\begin{aligned}
w(t) &= \sum_{k=0}^{N} a_k \cos\left(\frac{2\pi}{T} kt\right), \qquad \frac{-T}{2} < t < \frac{T}{2} \text{ (noncausal)} \\
w(t) &= \sum_{k=0}^{N} (-1)^k a_k \cos\left(\frac{2\pi}{T} kt\right), \qquad 0 < t < T \text{ (causal)} \qquad (7) \\
w(0) &= \sum_{k=0}^{N} a_k = 1, \qquad \text{scales peak of } w(t) \text{ to } 1.0
\end{aligned}
$$

Windows with two-term Fourier transforms include the HANN and HAMMING windows. When the two term coefficients $(a_0, a_1) = (0.5, 0.5)$, the window is the HANN window (often incorrectly called the HANNING window). It is also called the cosine-squared window. For these weights the highest side-lobe is 0.0267 or -31.47 dB below the peak main-lobe response and decays thereafter at 18 dB/octave. When the coefficients $(a_0, a_1) = (0.54, 0.46)$, the window is the HAMMING window. For these weights, the highest side-lobe is 0.00735 or -42.76 dB below the peak main-lobe response and decays thereafter at 6 dB/octave. We observe that we can realize over two orders of magnitude side-lobe level suppression by doubling the main-lobe width.

If additional side-lobe level suppression is desired, we have to increase the number of terms in the short cosine transform. Each new term increases the main-lobe width by placing another pair of $\text{sinc}(\pi fT)$ functions in the main-lobe. As the main-lobe bandwidth increases, we use the additional degrees of freedom to realize additional side-lobe level suppression. Examples of windows formed by the short cosine transforms and their respective side-lobe levels are shown in Table 1. The number of terms in the cosine series expansion represents the main-lobe width between the spectral peak and the first zero crossing of the main-lobe. Note that the coefficients listed here include the alternating signs, shown in the second option of Eq. (7), which forms causal windows.

The time and frequency responses of the windows listed in Table 1 are presented in Figs. 4 through 9. The windows contain 51 samples, a length selected to permit us to see some detail in their (1024) point Fourier transforms. The apparent modulation of the spectral side-lobes is an artifact due to the sampling grid bracketing the spectral zero crossings.

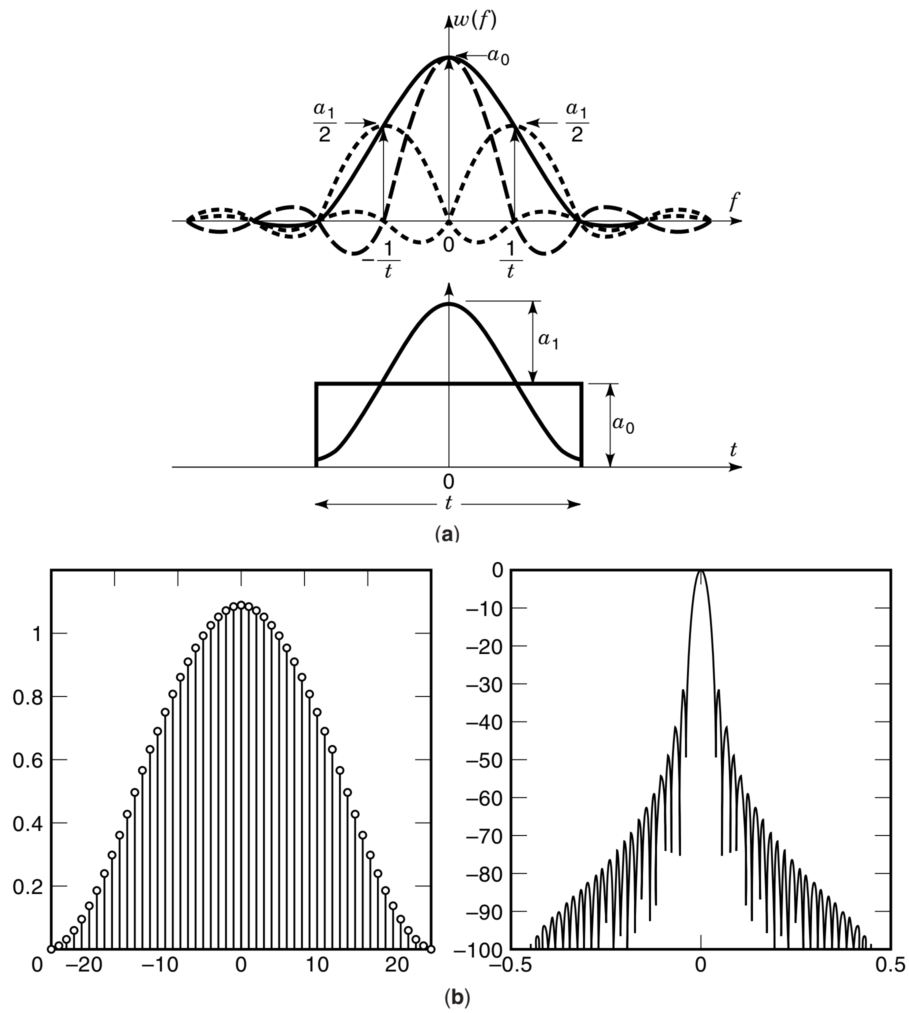

Figure 4. (a) Spectra and time description of a window formed as sum of rectangle and cosine. (b) Hann window and its Fourier transform.

WINDOWS WITH ADJUSTABLE DESIGN PARAMETERS

We recognize that windows trade spectral main-lobe width for spectral side-lobe levels. A good window achieves low side-lobe levels with minimum increase in main-lobe width. We now examine two windows that can make this trade in accord with an optimality criterion.

Table 1. Windows with Short Cosine Transforms

Name	Weights	Max Side-Lobe Level
Hann	$a_0 = 0.5$	−32 dB
	$a_1 = -0.5$	
Hamming	$a_0 = 0.54$	−43 dB
	$a_1 = -0.46$	
Blackman	$a_0 = 0.42$	−58 dB
(approximate)	$a_1 = -0.50$	
	$a_2 = 0.08$	
Blackman	$a_0 = 0.426\,591$	−68 dB
(exact)	$a_1 = -0.496\,561$	
	$a_2 = 0.076\,849$	
Blackman-Harris	$a_0 = 0.423\,23$	−72 dB
(3-term)	$a_1 = -0.497\,55$	
	$a_2 = 0.079\,22$	
Blackman-Harris	$a_0 = 0.358\,75$	−92 dB
(4-term)	$a_1 = -0.488\,29$	
	$a_2 = 0.141\,28$	
	$a_3 = -0.011\,68$	

Dolph-Chebyshev Window

The optimality criterion addressed by the Dolph-Chebyshev window is that its Fourier transform exhibits the narrowest main-lobe width for a specified (and selectable) side-lobe level. The Fourier transform of this window exhibits equal ripple at the specified side-lobe level. The Fourier transform of the window is a mapping of the Nth-order algebraic Chebyshev polynomial to the Nth-order trigonometric Chebyshev polynomial by the relationship $T_N(x) = \cos(N\theta)$. The Dolph-Chebyshev window is defined in terms of uniformly spaced samples of its Fourier transform. These samples are expressed as

$$W(k) = (-1)^k \frac{\cosh[N\cosh^{-1}(\beta\cos(\pi\, k/N))]}{\cosh[N\,\cosh^{-1}(\beta)]}, \qquad 0 \le k < N-1 \tag{8}$$

where

$$\beta = \cosh\left[\frac{1}{N}\cosh^{-1}(10^{-A/20})\right]$$

$$A = \text{side-lobe level (in dB)}$$

$$\mathrm{w(n)} = \sum^{N-1} W(k) e^{j\frac{2\pi}{N}nk}$$

$$W(N-k) = W(-k)$$

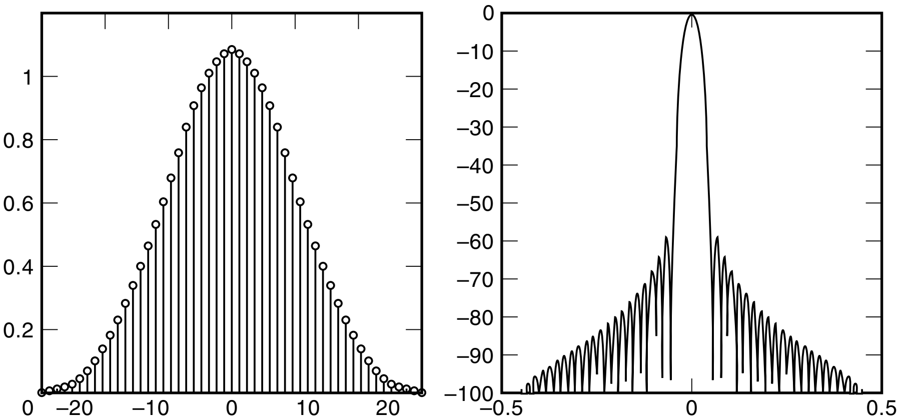

Figure 5. Hamming window and its Fourier transform.

Since the discrete Fourier transform is periodic on the unit circle, there is an end-point problem with the sample located at pi when the unit circle is cut at pi. It requires a slight modification of the relationship shown in Eq. (8). This modification is shown in the MATLAB code presented below. This code accomplishes the following tasks: First, reduce the number of sample points by one (from N to $N - 1$). Second, compute $N - 1$ spectral samples. Third, scale the first point by half and append a copy of this scaled sample to the opposite end of the spectral array, thus returning the array to the desired length N. Last, transform spectral samples to the time domain by an N-point DFT. This code is slightly simpler than the MATLAB code (*Chebwin*) used by the Signal Processing Toolbox and does not have the restriction that the size N be an odd integer.

```
function w=dolph(n,a)
% written by fred harris, SDSU,
n=n-1;
beta=cosh(acosh(10∧(abs(a)/20))/n);
arg=beta*cos(pi*(0:n-1)/n);
wf=cos(n*acos(arg));

w=real(fft((wf.*cos(pi*(0:n-1)))));
w(1)=w(1)/2; w=[w w(1)];
w=w/max(w);
```

The Fourier transform of this window exhibits uniform, or constant level side-lobes levels (inherited from the Chebyshev polynomial) and as such must contain impulses in its time series. These impulses are located at the window boundaries. When this window is used as a shading function in antennae systems, these impulses are not realizable, and their suppression results in an allied window known as the Taylor weighting. Figures 10 and 11 present the time and frequency description of a 40 dB side-lobe and an 80 dB side-lobe Dolph-Chebyshev window. The 40 dB window is included to demonstrate the end point impulses. As an aside, the Chebyshev, or equal-ripple behavior of the Dolph-Chebyshev window can be obtained iteratively by the Remez (or the equal ripple, or Parks-Mclellan) filter design routine. For comparison, Fig. 12 presents a window designed as a narrowband filter with 60 dB side-lobes. The MATLAB call for this design was

```
ww=remez(50,[0 .001 .047 0.5]/0.5,[1 1 0 0]).
```

The weights were scaled by ww(max) to set the maximum value of the window to unity. This filter, by virtue of the equal-ripple side-lobes, also exhibits end-point impulses.

A comment on system performance is called for at this point. Windows (and filters) with constant-level side-lobes, while optimal in the sense of equal ripple approximation, are suboptimal in terms of their integrated side-lobe levels. The window (or filter) is used in spectral analysis to reduce the signal bandwidth and then the sample rate. The reduction in the sample rate causes aliasing. The spectral content in the side-lobes (the out-of-band energy) folds back to the in-band interval and becomes in-band interference. A measure of this

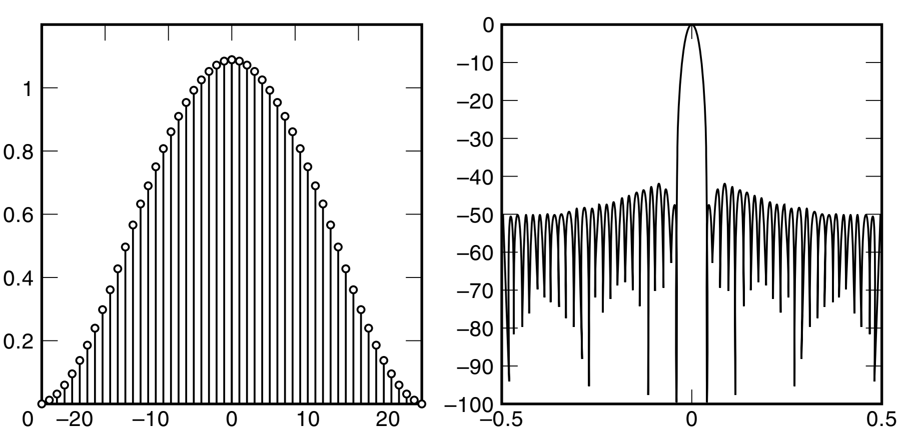

Figure 6. Blackman (approximate) window and its Fourier transform.

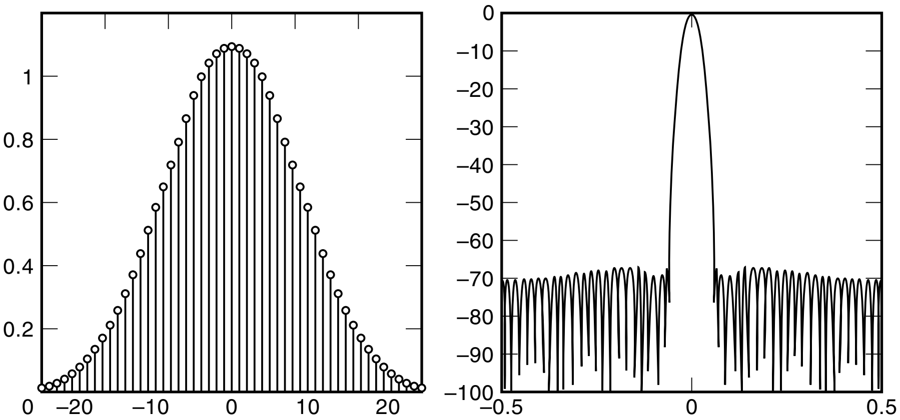

Figure 7. Blackman (exact) window and its Fourier transform.

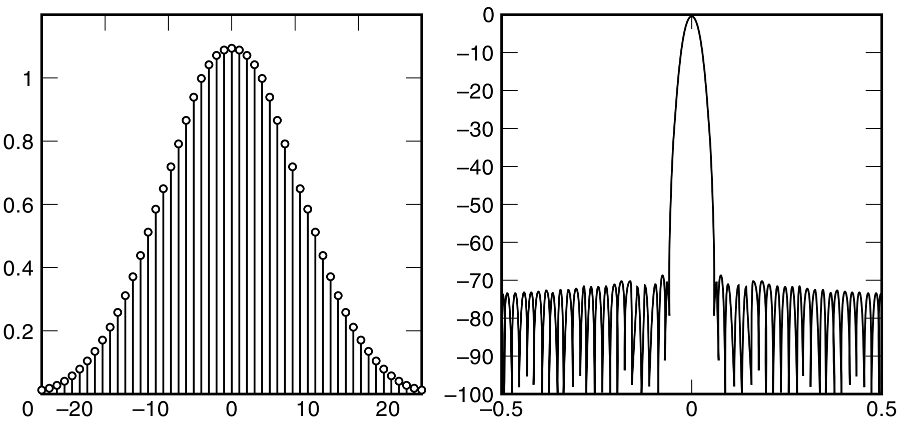

Figure 8. Blackman-Harris (3-term −67 dB) window and its Fourier transform.

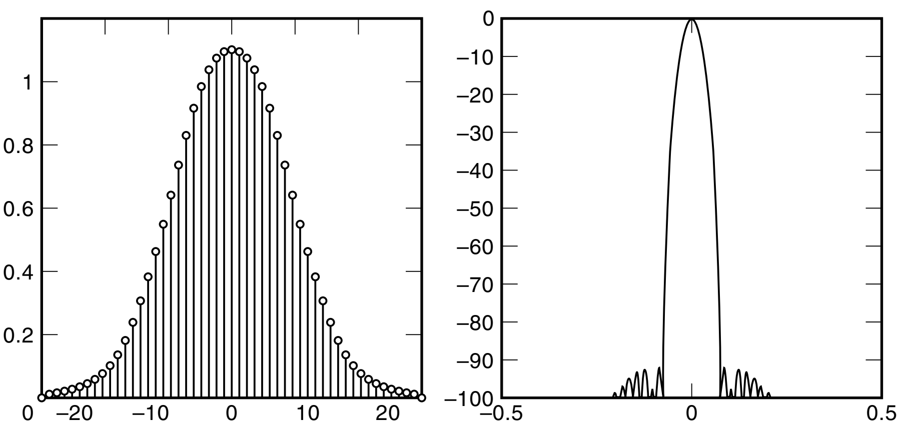

Figure 9. Blackman-Harris (4-term −92 dB) window and its Fourier transform.

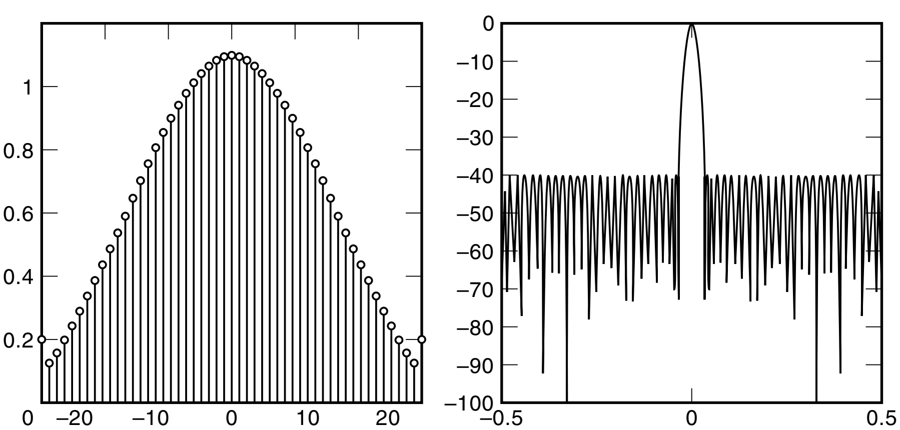

Figure 10. Dolph-Chebyshev (40 dB) window and its Fourier transform.

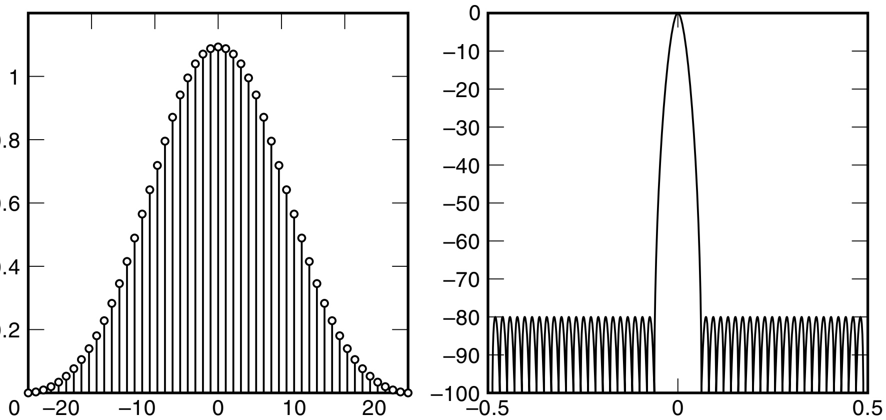

Figure 11. Dolph-Chebyshev (80 dB) window and its Fourier transform.

unexpected interference is integrated side-lobes which, for a given main-lobe width, is greater when the side-lobes are equal-ripple. From a systems viewpoint, the window (or filter) should exhibit 6 db per octave ($1/f$) rate of falloff of side-lobe levels. Faster rates of falloff actually increase integrated side-lobe levels because of an accompanying increase in close-in side-lobes as the remote side-lobes are depressed (while holding main-lobe width and window length fixed). System designers should shy away from equal-ripple windows (and filters).

Gaussian Window

A second window that exhibits a measure of optimality is the Gaussian or Weierstrass function. A desired property of a window is that they be smooth (usually) positive functions with Fourier transforms that approximate an impulse (i.e., tall thin main-lobe with low-level side-lobes). From the uncertainty principle we know that we cannot simultaneously concentrate both a signal and its Fourier transform. We can define the measure of concentration (or width) as the function's second central moments (i.e., moment of inertia). With σ_T being the RMS time duration and with σ_W being the RMS bandwidth (in hertz), we know these parameters must satisfy the uncertainty principle inequality

$$\sigma_T \sigma_W \geq \tfrac{1}{2} \tag{9}$$

The equality constraint is achieved only by the Gaussian function. Thus the Gaussian function, exhibiting a minimum time-bandwidth product, seems like a reasonable candidate for a window. Since windows span a finite support, when the Gaussian is used as a window, we must truncate or discard its tails. By restricting the window to a finite support the (truncated) Gaussian loses its minimum time-bandwidth distinction. Nevertheless, the window enjoys wide usage by virtue of its simplicity and (misplaced) reputation as a minimum time-bandwidth function.

The sampled Gaussian window is defined in Eq. (10) with the parameter α, the inverse of the standard deviation, controlling the effective time duration and the effective spectral width:

$$w(n) = \exp\left[-\frac{1}{2}\left(\alpha \frac{n}{N/2}\right)^2\right] \tag{10}$$

The Fourier transform of this truncated window is the convolution of the Gaussian transform with a Dirichlet kernel as indicated in Eq. (11). The convolution results in the formation of the spectral main-lobe (approximating the target's main-lobe) with accompanying side-lobes whose peak levels depend on the parameter α. As expected, the larger α leads to a wider main-lobe and lower side-lobes. Figures 13 and 14 present Gaussian windows with parameter a selected to achieve 60 and 80 dB side-lobe levels. Note that the main-lobes are considerably wider that those of the Dolph-Chebyshev and the upcoming Kaiser-Bessel windows. A useful observation is that the main-lobe of the Gaussian window is $\frac{1}{3}$ again wider than

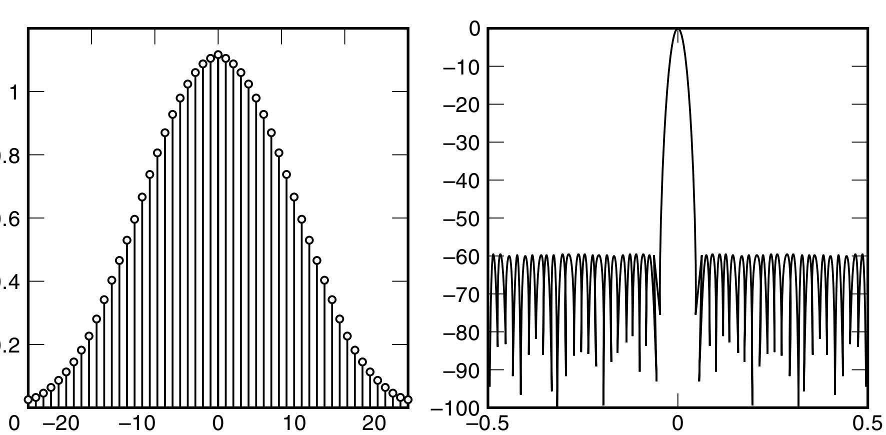

Figure 12. Remez algorithm low-pass filter/window (60 dB) and its Fourier transform.

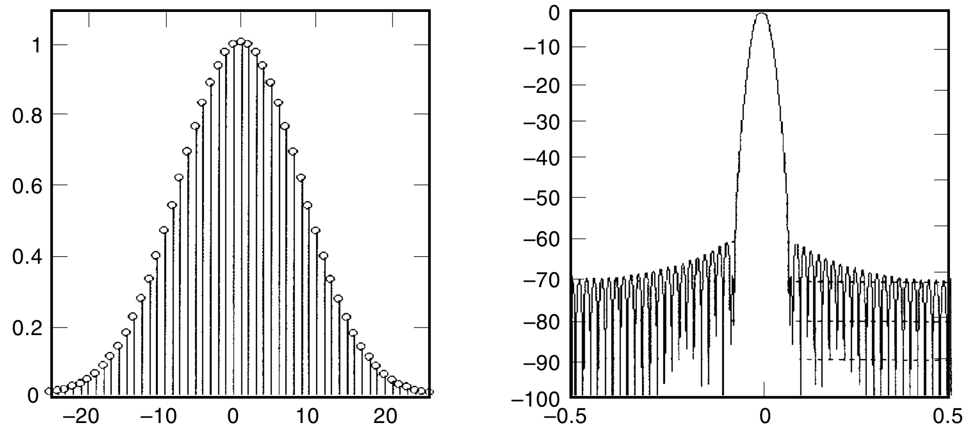

Figure 13. Gaussian (60 dB, $\alpha = 3.1$) window and its Fourier transform.

the Blackman-Harris window exhibiting the same side-lobe level.

Kaiser-Bessel Window

The last window we examine, designed in accord with an optimality criterion, is the Kaiser-Bessel (or prolate spheroidal wave) function. The previous two windows were characterized by minimum main-lobe width for a given side-lobe level and (hopefully) minimum bandwidth by approximately a minimum time-bandwidth product. Both windows had defects: One exhibited constant-level side-lobes (resulting in high-integrated side-lobes); the other exhibited excessive main-lobe width. An alternate, and related, optimality criterion is the problem of determining the wave-shape on a finite support that maximizes the energy in a specified bandwidth. This wave-shape has been identified by Slepian, Landau, and Pollak as the prolate spheroid function (of order zero) which contains a selectable time-bandwidth product parameter. Kaiser has discovered a simple numerical approximation to this function in terms of the zero-order modified Bessel function of the first kind (hence the designation Kaiser-Bessel). The Kaiser-Bessel window is defined in Eq. (11) where the parameter $\pi\alpha$ is the window's half time-bandwidth product. The series for the Bessel function converges quite rapidly due to the $k!$ in the denominator.

$$w(n) = \frac{I_0\left\{\pi\alpha\sqrt{1.0 - [n/(N/2)]}\right\}}{I_0[\pi\alpha]} \tag{11}$$

where

$$I_0(x) = \sum_{k=0}^{\infty}\left[\frac{(x/2)^k}{k!}\right]^2$$

The transform of the Kaiser-Bessel window (within very low-level aliasing terms) is the function shown in Eq. (12). We see that this function tends to sin x/x when the spectral argument is evaluated beyond the time-bandwidth related main-lobe bandwidth:

$$W(\theta) = \frac{N}{I_0(\alpha\pi)}\,\frac{\sinh\left[\sqrt{(\alpha\pi)^2 - (N\theta/2)^2}\,\right]}{\sqrt{(\alpha\pi)^2 - (N\theta/2)^2}} \tag{12}$$

Note that the Kaiser-Bessel window can also be approximated by samples of the main-lobe of its spectra, since the window is self-replicating under the time-limiting and band-limiting operations. That is, if $w(n)$ and $W(\theta)$ are a Fourier transform pair, then the band-limited version $\mathrm{Rect}(\theta/\alpha\ \pi)\cdot W(\theta)$ is a scaled version of $w(n)$. Similarly the transform of the band-limited spectra is a time series consisting of the original time-limited series $w(n)$ with appended side-lobe tails. Time limiting this new time series (truncating the tails) returns the pair back to their original relationship.

Figures 15 and 16 present the Kaiser-Bessel window for parameter $\alpha\pi$ selected to achieve 60 dB and 80 dB side-lobes. Compare the main-lobe widths to those of the earlier win-

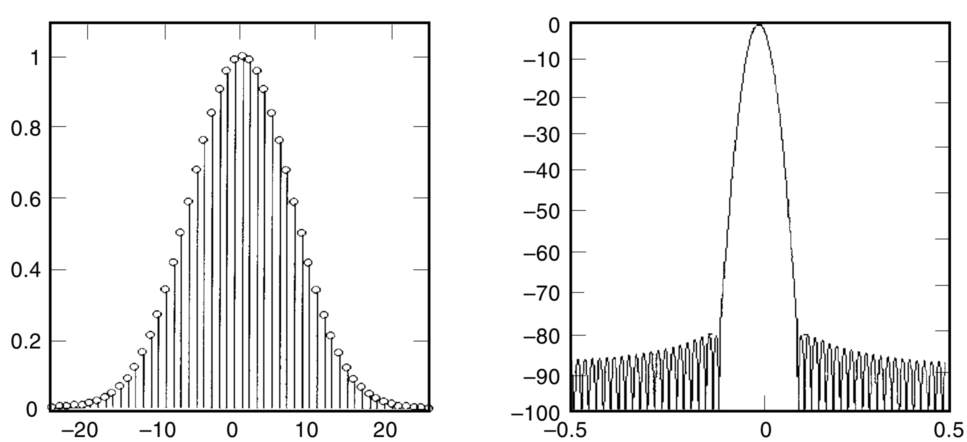

Figure 14. Gaussian (80 dB, $\alpha = 3.7$) window and its Fourier transform.

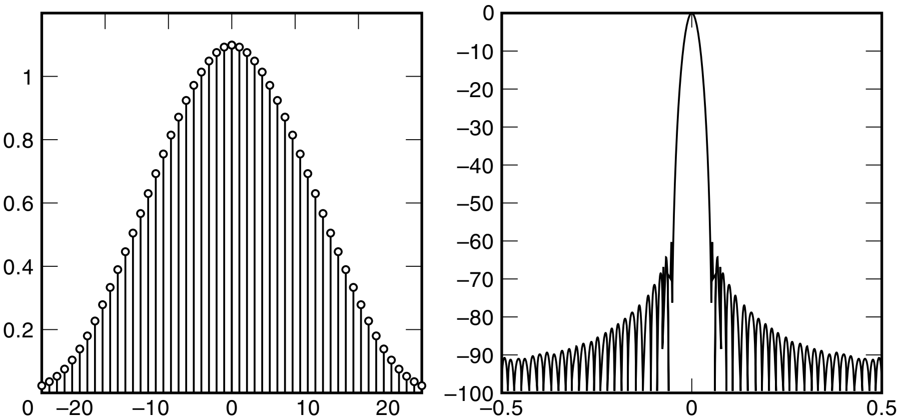

Figure 15. Kaiser-Bessel (60 dB, $\alpha\pi = 8.3$) window and its Fourier transform.

dows. As commented on earlier, windows can be designed using the Remez algorithm. When the penalty function of the Remez algorithm is made to increase linearly with frequency the side-lobes fall inversely with frequency (−6 dB/oct). Figure 17 presents a window designed by a modified Remez algorithm. The call to the modified routine is of the form

ww=remez(50,[0 .001 .0655 0.5]/0.5,[1 1 0 0],'slope = −1')

Note that due to the reduced side-lobe slope, this window exhibits a narrower main-lobe width compared to a Kaiser-Bessel with the same −80 dB side-lobe level.

SPECTRAL ANALYSIS AND WINDOW FIGURES OF MERIT

Windows are used in spectrum analysis to minimize additive biases caused by the artificial boundaries or discontinuities imposed on the time series being analyzed. We will now examine the incidental effects of the windows on the spectrum analysis process. In one use of a spectrum analyzer, we process a composite signal consisting of a sinusoid of interest, which we will consider the desired signal; we will consider other sinusoids not of interest as undesired interference and additive white noise. Figure 18 is a representation of the spectra of this signal set containing a single undesired line component described as

$$s(nT) = A_S\, e^{j\phi_S}\, e^{j\omega_S Tn} + A_U\, e^{j\phi_U}\, e^{j\omega_U Tn} + \mathscr{N}(nT) \tag{13}$$

The primary signal-processing tool used to perform spectrum analysis is the discrete Fourier transform (DFT). Consequently we will limit subsequent discussion of windows in spectral analysis to DFT based analysis. The DFT of the composite signal described in Eq. (13) will consist of three components as shown in Fig. 18 and as presented in Eq. (14). In this expression δk and Δk are the frequency displacements (in DFT bins) of the desired and undesired signal components from the DFT bin closest to the desired signal frequency. Recall that the DFT bin centers are located at integer multiples of the fundamental frequency $2\pi/NT$ radians/second defined by the support interval NT. Thus the sampled data frequency is defined by the index k with units of cycles per interval or by the equivalent sampled data frequency of $k(2\pi/N)$ radians/sample:

$$\begin{aligned} S(k) &= \sum_{n=0}^{N-1} w(n)s(n)e^{-j\frac{2\pi}{N}nk} \\ &= \sum_{n=0}^{N-1} w(n)[A_S\, e^{j\phi_S}\, e^{+j\frac{2\pi}{N}n(k+\delta k)} + A_U\, e^{j\phi_U} e^{+j\frac{2\pi}{N}n(k+\Delta k)} \\ &\quad + \mathscr{N}(n)]e^{-j\frac{2\pi}{N}nk} \end{aligned} \tag{14}$$

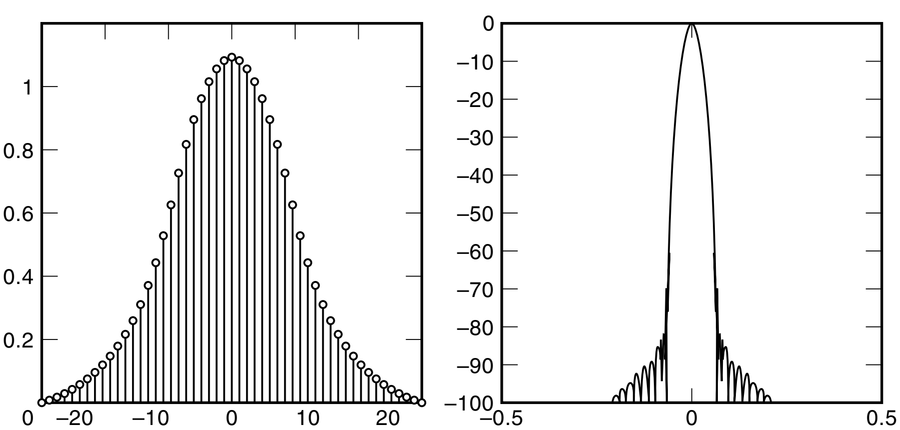

Figure 16. Kaiser-Bessel (80 dB, $\alpha\pi = 10.7$) window and its Fourier transform.

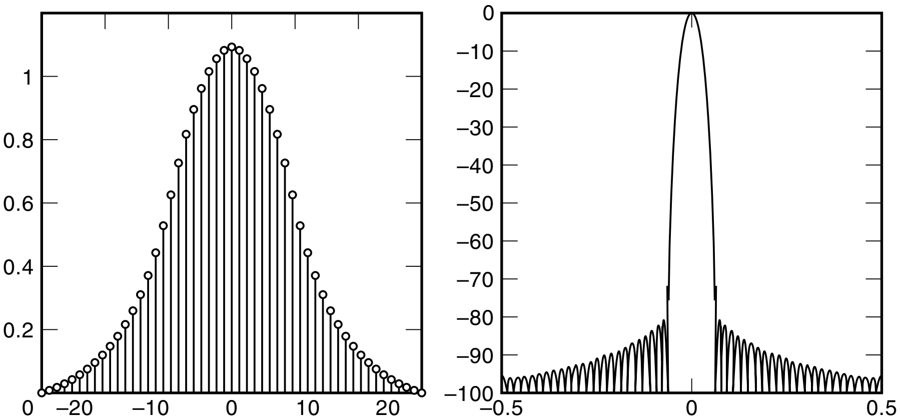

Figure 17. Remez algorithm (80 dB, −6 dB/oct) window/filter and its Fourier transform.

The three separate components of the DFT presented in Eq. (14) are identified as

$$
\begin{aligned}
S(k)_{\text{DES SIG}} &= \sum_{n=0}^{N-1} w(n) A_S\, e^{j\phi_S} e^{+j\frac{2\pi}{N}n(k+\delta k)}\, e^{-j\frac{2\pi}{N}nk} \\
&= A_S\, e^{j\phi_S} \sum_{n=0}^{N-1} w(n) e^{+j\frac{2\pi}{N}n\delta k} \\
&= A_S\, e^{j\phi_S}\, W(\delta k) \\
S(k)_{\text{UNDES SIG}} &= \sum_{n=0}^{N-1} w(n) A_U\, e^{j\phi_U}\, e^{+j\frac{2\pi}{N}n(k+\Delta k)}\, e^{-j\frac{2\pi}{N}nk} \qquad (15) \\
&= A_U\, e^{j\phi_U} \sum_{n=0}^{N-1} w(n) e^{+j\frac{2\pi}{N}n\Delta k} \\
&= A_U\, e^{j\phi_U}\, W(\Delta k) \\
S(k)_{\text{NOISE}} &= \sum_{n=0}^{N-1} w(n) \mathcal{N}(n) e^{-j\frac{2\pi}{N}nk}
\end{aligned}
$$

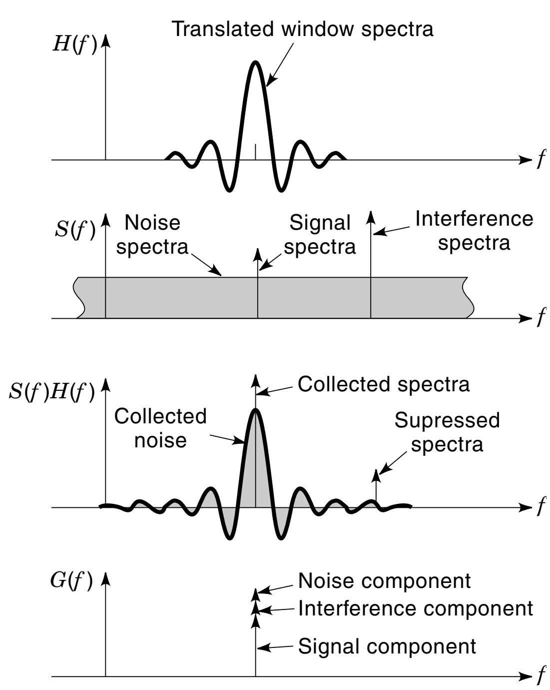

Figure 18. Graphical representation of spectra interacting with observation window.

The signal component, $S(k)_{\text{DES SIG}}$, of the DFT output is seen to preserve the complex amplitude of the input sinusoid but multiplies that amplitude by a gain term, which we recognize as the DFT of the window. The DFT is evaluated at δk, the frequency displacement of the input sinusoid from the nearest DFT bin. We note that the frequency response of the window spectra centered at the kth bin and observed by the input sinusoid at frequency $k + \delta k$ cycles/interval is the same as the frequency response of the window centered at DC and observed at frequency offset δk. When the displacement, δk, is zero this gain defaults to the DC (or zero frequency) response of the window. This gain is called the peak amplitude gain of the window and, as shown in Eq. (16), is the sum of the window weights. This sum is bounded by N (for the rectangle window) and is a_0N for the short cosine transforms (see Section entitled Windows as a Sum of Cosines). For good windows, typical values of peak amplitude gain is on the order of $0.5 * N$ through $0.35 * N$. A related gain term is called the peak power gain of the window which is expressed as

$$
\begin{aligned}
\text{Peak signal gain} &\equiv W(0) = \sum_{n=0}^{N-1} w(n) \\
\text{Peak signal power gain} &\equiv W^2(0) = \left[\sum_{n=0}^{N-1} w(n)\right]^2
\end{aligned}
\qquad (16)
$$

The undesired component, $S(k)_{\text{UNDES SIG}}$, of the DFT output is also seen to preserve the complex amplitude of the input sinusoid but multiplies that amplitude by a gain term $W(\Delta k)$. We recognize the gain term as the DFT of the window evaluated at Δk, the frequency displacement of the undesired input sinusoid from the DFT bin of interest. This term is the spectral leakage term or out-of-band frequency response of the window. It is our desire to control this term which motivated us to design and use good windows. When Δk is greater than the window's main-lode width (3 to 6 bins), this term is the window's side-lobe levels, which can be on the order of $0.01 * N$ through $0.0001 * N$.

The component $S(k)_{\text{NOISE}}$ is the DFT of the input noise. We can assume that this noise is zero mean and white with variance $\sigma^2_{\mathcal{N}}$. Since the noise in a random variable, so is it's DFT, so we are obliged to describe the DFT of the noise by its statistics. Two statistics of primary interest are the first and second moments:

$$E\{S_{\rm NOISE}(k)\} = E\left\{\sum_{n=0}^{N-1} w(n)\mathcal{N}(n)e^{j\frac{2\pi}{N}nk}\right\}$$
$$= \sum_{n=0}^{N-1} w(n)E\{\mathcal{N}(n)\}e^{-j\frac{2\pi}{N}nk}$$
$$= 0$$

$$E\{|S_{\rm NOISE}(k)|^2\} = E\left\{\sum_{n_1=0}^{N-1}\sum_{n_2=0}^{N-1} w(n_1)w^*(n_2)\mathcal{N}(n_1)\mathcal{N}^*(n_2)e^{-j\frac{2\pi}{N}n_1k}e^{+j\frac{2\pi}{N}n_2k}\right\} \tag{17}$$
$$= \sum_{n_1=0}^{N-1}\sum_{n_2=0}^{N-1} w(n_1)w^*(n_2)E\{\mathcal{N}(n_1)\mathcal{N}(n_2)\}e^{-j\frac{2\pi}{N}(n_1-n_2)k}$$
$$= \sum_{n=0}^{N-1} w^2(n)\sigma^2_{\mathcal{N}}$$
$$= \sigma^2_{\mathcal{N}}\sum_{n=0}^{N-1} w^2(n)$$

We see that the DFT output variance, due to input noise, is a scaled version of the input noise variance. The scale term is the sum of square of the window weights. This gain, shown in Eq. (18), is termed the peak noise power gain of the window. This is of course bounded by N (for the rectangle) and is on the order of $(\frac{3}{8})\,N$ for other windows:

$$\text{Peak noise power gain} \equiv \text{NPG} = \sum_{n=0}^{N-1} w^2(n) \tag{18}$$

Figures of Merit

The use of a window leads to conflicting effects on the output of the transform. The window is applied to data to suppress out-of-band side-lobe levels. This is a desirable effect. The window controls side-lobes by smoothly discarding data near the boundaries of the observation interval. This has the effect of reducing the amplitude, hence energy, of both signal and noise components presented to the transform. Concurrently the increased bandwidth of the window's spectral main-lobe (required to purchase the reduced side-lobe levels) permits additional noise into the measurement.

To facilitate comparison of different windows, we define two performance measures related to the effects of the window on both signal and noise. The first of these is equivalent noise bandwidth (ENBW). This parameter indicates the equivalent rectangular bandwidth of a filter with the same peak gain of the filter that would result in the same output noise power. ENBW is illustrated in Fig. 19 and is computed by dividing the total energy collected by the window by the peak power gain of the window:

$$\text{ENBW} = \frac{\sum_{n=0}^{N-1} w^2(n)}{\left[\sum_{n=0}^{N-1} w(n)\right]^2} \tag{19}$$

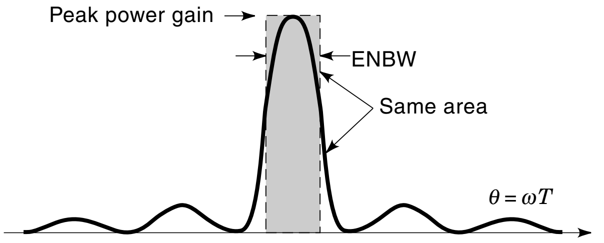

Figure 19. Equivalent noise bandwidth (ENBW): Area under power gain curve allocated to rectangle of same amplitude.

We note that the rectangle window has the smallest ENBW of $1/N$, while a Hann window has an ENBW of $1.5/N$. The units of ENBW are spectral bins, and the larger ENBW indicates an increased variance of a spectral measurement. It is common practice to normalize the ENBW of the particular window of length N to the ENBW of the rectangle of the same length. Thus the normalized ENBW of the Hann window is 1.5 bins A table of popular windows along with their ENBW is presented at the end of this section.

A related figure of merit for a windowed DFT is the processing gain (PG) or improvement in signal-to-noise ratio obtained when using the window. This improvement is the ratio of output SNR to input SNR of a noisy sinewave. Processing gain can be as large as N (for a rectangle) and is usually on the order of $0.4N$ for windows with good side-lobe levels. The processing gain is also equal to the reciprocal of the window's ENBW:

$$\text{SNR}_{\rm OUT} = \frac{A^2\left[\sum_{n=0}^{N-1} w(n)\right]^2}{\sigma^2_{\mathcal{N}}\sum_{n=0}^{N-1} w^2(n)}$$
$$\text{SNR}_{\rm IN} = \frac{A^2}{\sigma^2_{\mathcal{N}}} \tag{20}$$
$$\text{PG} = \frac{\text{SNR}_{\rm OUT}}{\text{SNR}_{\rm IN}} = \frac{\left[\sum_{n=0}^{N-1} w(n)\right]^2}{\sum_{n=0}^{N-1} w^2(n)} = \frac{1}{\text{ENBW}}$$

Scalloping Loss. The amplitude gain of a windowed transform applied to a sinusoid located at bin $k + \delta k$ was presented in Eq. (16) and is repeated here in Eq. (21). The amplitude gain $W(\delta k)$ is a function of the frequency offset, δk, of the input sinusoid from the processed bin. This

$$S_{\rm DES\,SIG}(k) = \sum_{n=0}^{N-1} w(n)A_S\,e^{j\phi_S}\,e^{j\frac{2\pi}{N}(k+\delta k)n}\,e^{-j\frac{2\pi}{N}kn}$$
$$= A_S\,e^{j\phi_S}\sum_{n=0}^{N-1} w(n)e^{j\frac{2\pi}{N}\delta kn} \tag{21}$$
$$= A_S\,e^{j\phi_S}\,W(\delta\,k)$$

frequency-dependent gain due to the offset from the DFT bin center represents a reduction in processing gain and is known as scalloping loss. The structure of the frequency-dependent gain can be visualized with the aid of Fig. 20.

As shown in Fig. 20, when a sinusoidal input frequency is located in the center of a particular DFT bin, the pair of filters bracketing this bin respond with equal amplitudes. If the center frequency of an input sinusoid is shifted from the bin cen-

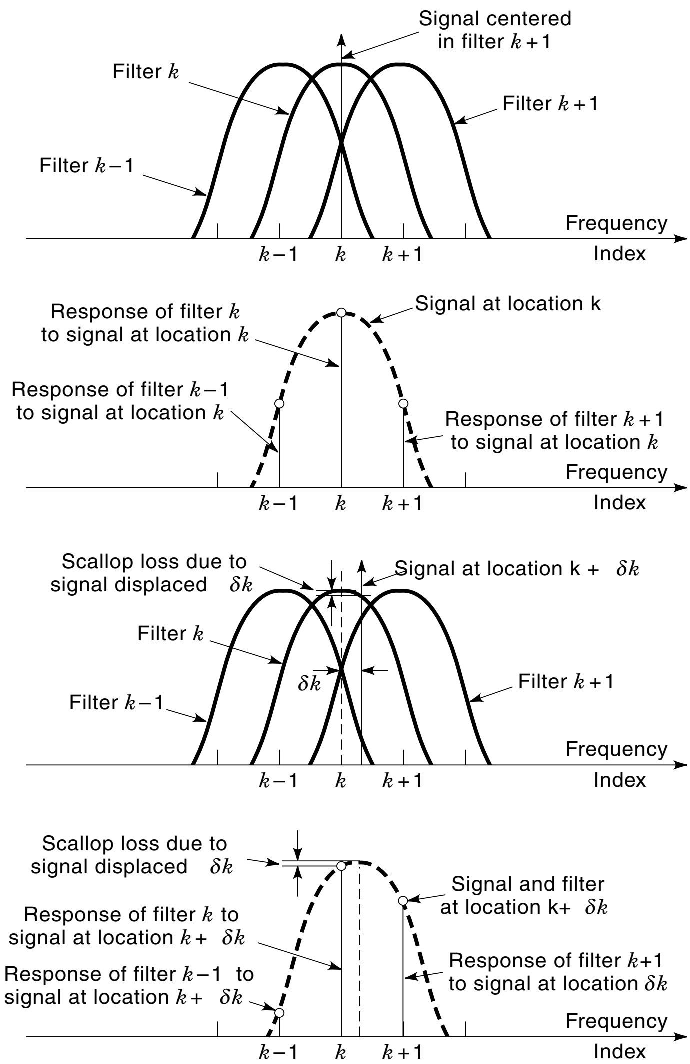

Figure 20. Scalloping loss: Reduction in spectral response of DFT filters to bin-centered and non-bin-centered spectral line.

ter of filter k toward filter $k + 1$, the amplitude response of filter $k - 1$ and filter k drops, and the response of the filter $k + 1$ is increased. This drop in amplitude is scalloping loss. When the sinusoid is located at the midpoint between two filters, say at $k + \frac{1}{2}$, the two bracketing filters, k and $k + 1$, respond with the same amplitude. This amplitude corresponds to the maximum reduction in filter response and is called the peak scallop loss. When the peak scallop loss is presented in decibels, it represents the maximum reduction in signal to noise ratio of a windowed transform due to spectral position of input signals. Note that the signal can never be located, more than $\frac{1}{2}$ a bin from some center frequency. The rectangle window, due to its very narrow main-lobe width, exhibits the maximum scallop loss of −3.9 dB. Windows with deeper side-lobe levels have wider main-lobes and consequently exhibit reduced scalloping loss typically on the order of 1.0 dB.

If scalloping loss is an important consideration, it can be significantly reduced by zero-extending the windowed data and performing a double-length transform. The loss then corresponds to a $\frac{1}{4}$ bin shift of the original spectral analysis. An alternate technique is to modify the window so that it is has a flat spectral width between bin centers. This modification of the window criterion results in windows with negative weights and a significant increase in ENBW of the filter. We have used this form of a window, called the Harris flattop in a number of spectrum analyzers used as frequency-dependent voltmeters (for use in acceptance testing procedures). The parameters of this window are presented in the figure of merit table, and Fig. 21 presents the time and frequency response of the window along with a detailed view of its scallop loss.

Overlap Correlation. When the DFT is used to obtain power spectral estimates of random stationary processes, an ensemble of spectral measurements is averaged to reduce the variance of the estimates. The signal flow for this process is shown in Fig. 22, where we see the input data are buffered, windowed, and transformed to form the spectral description of the input data blocks. The transform is converted to a raw (two degrees of freedom) estimate of power spectrum by a conjugate product and converted to a smoothed (higher degrees of freedom estimate) by averaging a number of raw power estimates.

When the successive transforms are obtained from non-overlapped segments of the time series, the standard deviation of the spectral estimates obtained by simple averaging is reduced by the square root of the number of averages. For instance, averaging 32 independent transforms will reduce the standard deviation by a factor of 5.6 or 15 dB. Figure 23 demonstrates the improvement in variance obtained by the ensemble averaging of independent transforms. We apply windows to data to suppress artificial discontinuities at the data boundaries. The window essentially discards the data in the intervals nears near the boundaries. To avoid missing data, we overlap successive intervals and obtain what has been called the sliding windowed DFT. Typical values of interval overlap for successive transforms are 75% and 50%. These overlap intervals are often called 4-to-1 overlaps and 2-to-1 overlaps, respectively. The data collected from successive overlapped and windowed transforms are not independent. Consequently the amount of variance reduction obtained by ensemble averaging of spectra will be significantly reduced.

The variance reduction obtained by averaging correlated data can be easily determined by examining the terms in the covariance matrix of the summation as

$$\sigma_{\mathrm{AVG}}^2 = E\left\{\left[\frac{1}{N}\sum_{n=0}^{N-1} p(n)\right]^2\right\}$$
$$= \frac{1}{N^2}\,\text{SUM OF ENTRIES}$$
$$\begin{bmatrix} r(0) & r(1) & r(2) & \cdots & r(N-1) \\ r(-1) & r(0) & r(1) & \cdots & r(N-2) \\ r(-2) & r(-1) & r(0) & \cdots & r(N-1) \\ \ddots & \ddots & \ddots & & \ddots \\ r(-N+1) & r(-N+2) & r(-N+3) & \cdots & r(0) \end{bmatrix} \tag{22}$$

When the entries in the summation of Eq. (22) are independent, the diagonal terms of the covariance matrix are the only nonzero terms, and the summation collapses to $c(0)/N$. When the collected data represent 50% overlapped intervals, the

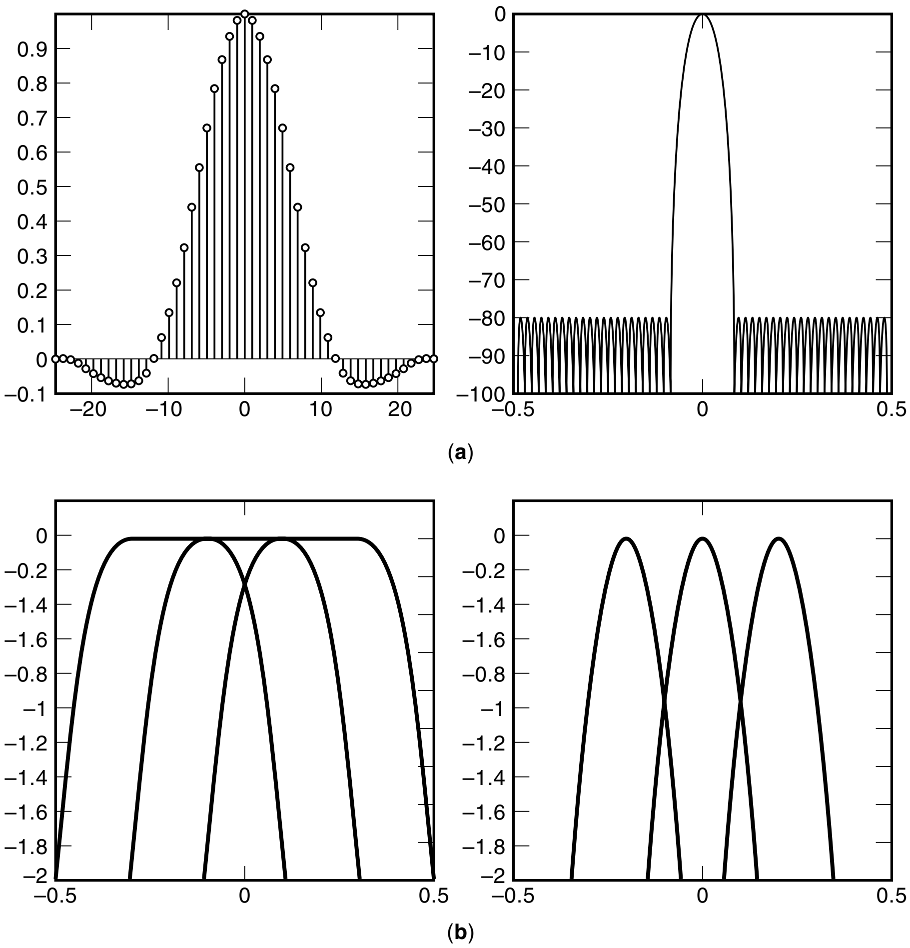

Figure 21. (a) Harris flattop window and its Fourier transform. (b) Scallop response of three adjacent DFT bins for −80 dB Harris flattop window and for −80 dB Dolph-Chebyshev window.

matrix becomes banded and contains only the diagonal terms and the first upper and lower off-diagonal terms. Gathering all the terms on the three diagonals results in the summation

$$\sigma^2_{\mathrm{AVG}}(0.50-OL)=\frac{1}{N}[r(0)+2r(0.5)]-\frac{2}{N^2}[r(0.5)] \qquad (23)$$

When the collected data represent 75% overlapped intervals, the matrix becomes banded and contains only the diagonal terms and the three upper and lower off-diagonal terms. Gathering all the terms on the seven diagonals results in the summation

$$\begin{aligned}\sigma^2_{\mathrm{AVG}}(0.75-OL)=&\frac{1}{N}[r(0)+2r(0.75)+2r(0.50)+2r(0.25)]\\&-\frac{2}{N^2}[r(0.75)+2r(0.50)+3r(0.25)]\end{aligned} \qquad (24)$$

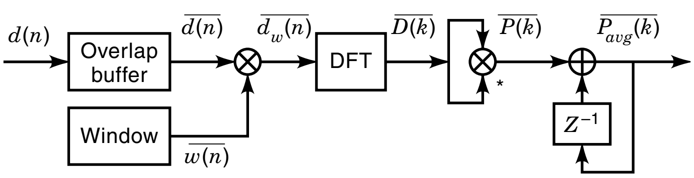

Figure 22. Estimating power spectrum as average of overlapped and windowed DFTs.

The correlation coefficients presented in Eqs. (23) and (24) are related to the normalized coefficients of correlation as

$$r(x)=c^2(x)r(0)=c^2(x)\sigma_p^2 \qquad (25)$$

Substituting Eq. (25) into Eqs. (23) and (24) results in Eq. (26), the expressions derived by Walsh:

$$\sigma^2_{\mathrm{AVG}}(0.50-OL)=\sigma_P^2\left[\frac{1}{N}[1+2c^2(0.50)]-\frac{2}{N^2}[c^2(0.50)]\right]$$

$$\sigma^2_{\mathrm{AVG}}(0.75-OL)=\sigma_P^2\left[\begin{array}{l}\frac{1}{N}[1+2c^2(0.75)+2c^2(0.50)+2c^2(0.25)]\\-\frac{2}{N^2}[c^2(0.75)+2c^2(0.50)+3c^2(0.25)]\end{array}\right] \qquad (26)$$

The correlation coefficients required to evaluate Eq. (26) are listed in Table 2 for many useful windows.

How Much Overlap?

Windows are applied to a sequence of overlapped intervals to form the sliding windowed DFT. When the data are stationary, an ensemble average can be performed to improve statistics of the spectral estimates. As observed in the previous sec-

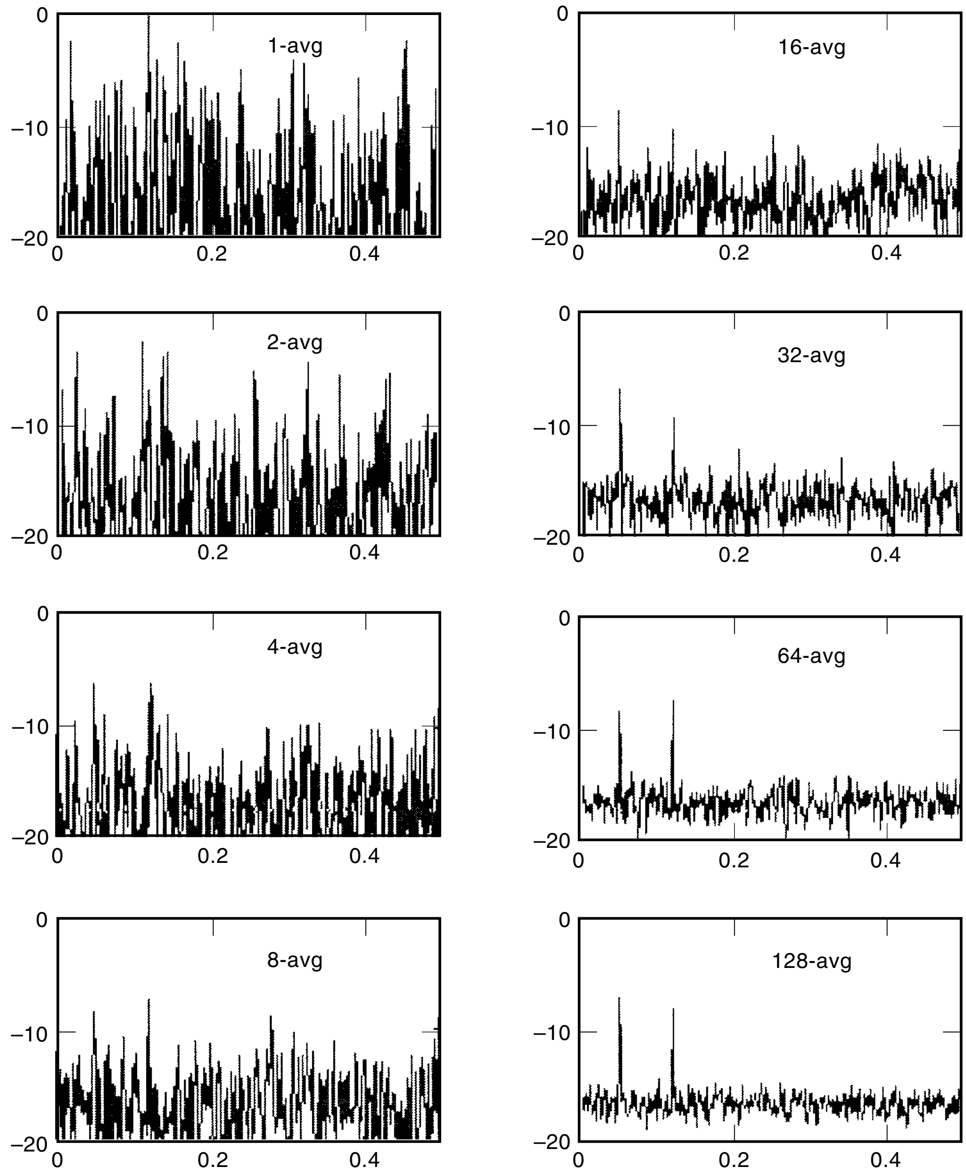

Figure 23. Ensemble averages of power spectra demonstrating need for variance reduction and rate of reduction with increased number of terms.

tion, the overlapped windows deliver correlated spectral estimates to the averager, and the variance reduction is no longer proportional to the square root of the number of averages. A question we address here is how much overlap should we apply to the succession of windows and what effect does the percent overlap have on the stability of the resulting spectral estimate.

The overlap process is indicated in Fig. 24. When a smooth window is applied to a data observation interval, the suppressed data near the boundaries are recovered by overlapping successive intervals. To determine the required amount of overlap, we can view the window as a filter that limits the bandwidth of the output signal and then invoke the Nyquist criterion to match the output sample rate to the output bandwidth. The Fourier transform of the typical window and the required spectral spacing to maintain a clear spectral region is shown in Fig. 25. The window main-lobe bandwidth, between the peak and first zero crossing, widens as the side-lobe structure is reduced by modulating the time envelope. To prevent the main-lobe spectra from aliasing back into the DFT bin, the replicates of the main-lobe must be separated by its lobe width plus a half a bin-width. For instance, the main-lobe width for a rectangle window is 1 DFT bin (f_s/N). To keep the main-lobe from folding back in-band (above the -13.5 dB side-lobe levels), the spectral copies must be separated by 1.2 bins. Thus the required sample rate is $1.25 * f_s/N$. This output rate is achieved by taking 1 output for every $0.8N$ inputs, which corresponds to 20% overlapped rectangle weighting. Similarly the Hann and Hamming windows have a main-lobe bandwidth of 2 DFT bins, so the required spectral separation, hence sample rate, is approximately $2.5 * f_s/N$. This output rate is achieved by taking 1 output for every $N/2.5$ inputs, which corresponds to 60% overlap of successive windows. The actual overlap is slightly smaller due to allowing a section of the main-lobe below side-lobe level to alias back into band. Table 3 presents common windows and their required overlap. In practice, actual overlap amounts are chosen to be convenient intervals such as 50% or 75%.

When we window and overlap transforms, we recognize that the windowed spectra exhibits a higher variance due to

Table 2. Figures of Merit for Common Windows

Window	Maximum Side-Lobe (dB)	Side-Lobe Slope (dB/OCT)	Coherent Gain	ENBW (bins)	Scallop Loss (dB)	Overlap Correlation 4–1	Overlap Correlation 2–1
Rectangle	−13.4	−6	1.000	1.000	−3.92	0.750	0.500
Triangle	−26.5	−12	0.500	1.333	−1.83	0.719	0.250
Hann	−31.5	−18	0.500	1.500	−1.43	0.659	0.167
Hamming	−42.7	−6	0.540	1.364	−1.75	0.707	0.234
Exact Blackman	−67.6	−6	0.426	1.693	−1.15	0.578	0.100
Blackman	−58.2	−18	0.420	1.727	−1.10	0.567	0.090
Gaussian							
$\alpha = 2.46$	−40.0	−6	0.502	1.427	−1.62	0.679	0.202
$\alpha = 3.15$	−60.0	−6	0.397	1.784	−1.06	0.537	0.081
$\alpha = 3.76$	−80.0	−6	0.333	2.123	−0.75	0.413	0.029
Dolph-Chebyshev	−40.0	0	0.589	1.304	−2.06	0.719	0.286
	−60.0	0	0.479	1.518	−1.42	0.646	0.161
	−80.0	0	0.414	1.743	−1.09	0.559	0.087
Kaiser-Bessel							
$\alpha = 5.47$	−40.0	−6	0.522	1.412	−1.62	0.700	0.208
$\alpha = 8.15$	−60.0	−6	0.431	1.681	−1.16	0.584	0.103
$\alpha = 10.66$	−80.0	−6	0.379	1.903	−0.09	0.498	0.053
Remez (−80 dB)	−80.0	−6	0.407	1.773	−1.05	0.547	0.079
Harris flattop (−80 dB)	−80.0	0	0.234	3.495	−0.01	0.102	−0.031
Blackman-Harris Minimum 3-term	−71.0	−6	0.423	1.791	−1.13	0.572	0.096
Blackman-Harris Minimum 4-term	−92.0	−6	0.359	2.004	−0.83	0.460	0.038

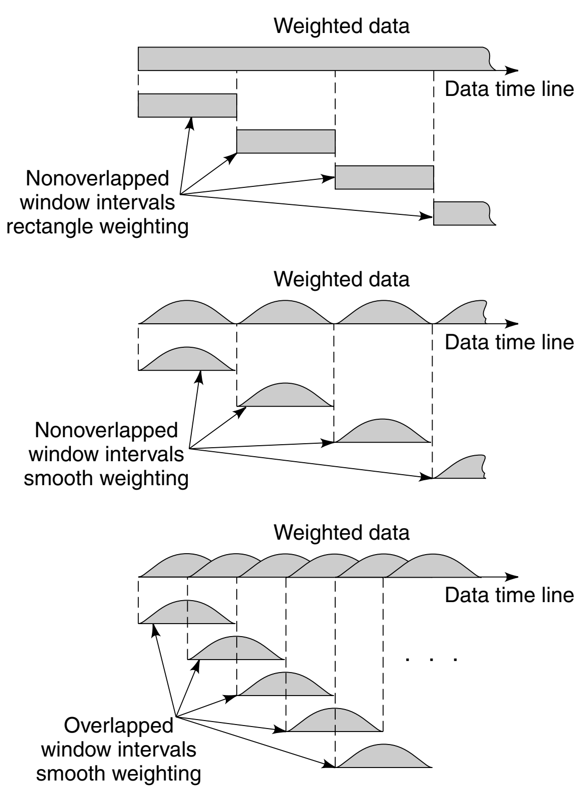

Figure 24. Partition of time line to nonoverlapped and overlapped window segments.

the increased ENBW associated with the window. The reduction in variance improvement was alluded to in Eq. (26) and is repeated in slightly altered form

$$\frac{1}{N_{\mathrm{EFFECTIVE}}} = \frac{1}{N_{\mathrm{AVG}}}\left[1 + \sum_{n=1}^{N_{\mathrm{AVG}}}\left(1 - \frac{n}{N_{\mathrm{AVG}}}\right)c^2(ns)\right] \tag{27}$$

Here the parameter s is the fractional shift of the overlapped intervals, $c(s)$ is the normalized correlation coefficient, N_{AVG} is the number of overlapped intervals spanning the data processing interval, and $N_{\mathrm{EFFECTIVE}}$ is the equivalent number of independent terms in the averaging process. We note that a small amount of shift, s, is equivalent to a large overlap ($OL = 1 - s$) and that large overlap intervals implies high correlation and little improvement in variance due to averaging. Conceptually the overlapped windows offer additional terms to the averager that uses the additional terms to reduce the variance. With additional increase in overlap, the averaging improvement saturates due to the high correlation of the data.

Table 4 lists the actual number of intervals for various amounts of overlap for a data set, which spans 32 nonoverlapping intervals. Figure 26 demonstrates how the effective number of terms initially increases with percent increased overlap and then saturates as the overlap increases the correlation of successive intervals. For this example the length of the data interval corresponded to 32 contiguous blocks. Note that even the rectangle window offers additional variance reduction with overlapped processing.

Observe that in Fig. 26 the N_eff curves for the different windows saturate at different amounts of overlap and that this overlap corresponds to the percent overlap listed in Table

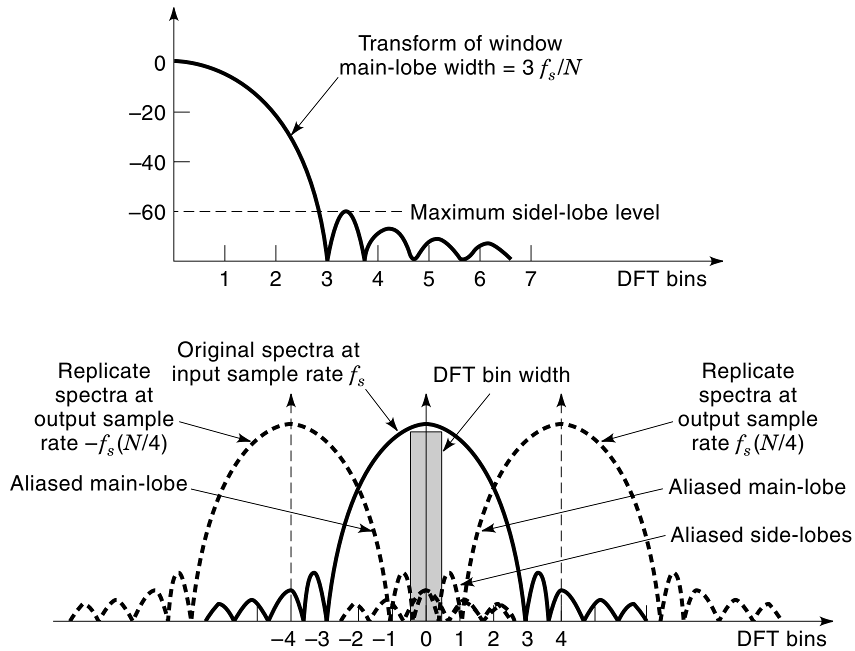

Figure 25. Window bandwidth and spectral replicates at output sample rate.

Table 3. Windows and Optimum Overlap Widths Required to Satisfy Nyquist

Window	Aliasing Level	Overlap	
		Percent	Shift
Rectangle	−13.4 dB	20.0%	$0.80N$
Triangle	−26.8 dB	52.0%	$0.48N$
Hann	−31.5 dB	56.0%	$0.44N$
Hamming	−42.7 dB	56.0%	$0.44N$
Blackman	−58.2 dB	69.0%	$0.31N$
Gaussian			
$\alpha = 2.46$ (−40 dB)	−40.0 dB	70.0%	$0.30N$
$\alpha = 3.15$ (−60 dB)	−60.0 dB	76.0%	$0.24N$
$\alpha = 3.76$ (−80 dB)	−80.0 dB	83.0%	$0.17N$
Dolph-Chebyshev	−40.0 dB	44.0%	$0.56N$
	−60.0 dB	67.0%	$0.33N$
	−80.0 dB	74.0%	$0.26N$
Kaiser-Bessel			
$\alpha = 5.47$ (−40 dB)	−40.0 dB	40.0%	$0.60N$
$\alpha = 8.15$ (−60 dB)	−60.0 dB	70.0%	$0.30N$
$\alpha = 10.66$ (−80 dB)	−80.0 dB	75.0%	$0.25N$
Harris-flattop (−80 dB)	−80.0 dB	78.0%	$0.22N$
Blackman-Harris Minimum 3-term	−71.0 dB	70.0%	$0.30N$
Blackman-Harris Minimum 4-term	−92.0 dB	76.0%	$0.24N$

Table 4. Number of Overlapping Intervals Spanning 32 Nonoverlapped Intervals

OL	0/8	1/8	2/8	3/8	4/8	5/8	6/8	7/8
N_{AVG}	32	36	42	51	64	85	128	256

3 determined by the Nyquist criterion applied to the mainlobe of the window's spectra. An interesting observation is that the ratio of the saturated N_eff of each window to the N_eff of the rectangle window at the same overlap for which the curve saturates is the ENBW of that window. Conversely, the saturated processing gain of each window divided by the window's ENBW is the N_eff of the rectangle window operating at the same level of overlap. This relationship is demonstrated in Table 5 for the various windows of Fig. 26. This is an important observation. It tells us that the increase in spectral variance due to the wider bandwidth of the window (applied to succession of time intervals) is precisely canceled by the increased processing gain offered by the overlap processing.

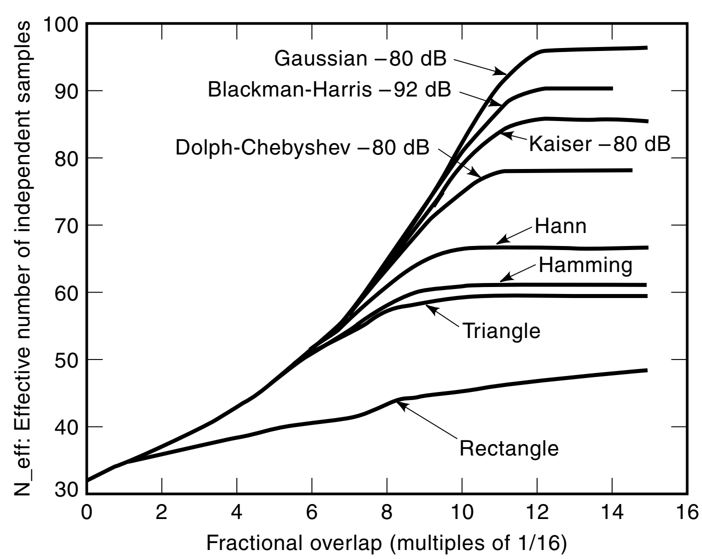

Figure 26. Effective number of independent samples obtained from processing windowed and overlapped blocks.

Table 5. Comparison of Effective Number of Independent Measurements to ENBW of Various Windows

Window	N_eff(Sat)	ENBW	Ratio
Gaussian	97	2.123	45.7
Blackman-Harris	91	2.004	45.4
Kaiser (−80 dB)	86	1.903	45.2
Dolph-Chebyshev (−80 dB)	78	1.743	44.7
Hann	67	1.500	44.7
Hamming	61	1.364	44.7
Triangle	60	1.333	45.0

A final comment about the efficiency of overlapped processing is related to Fig. 27. Here the ratio of the effective number of transforms obtained by overlapped processing is compared to the actual number of transformed performed. When the ratio is close to unity, the additional processing is offering additional processing gain. When the ratio is significantly less than unity, say 0.9, then the improvement in SNR is not increasing as fast as the workload, and we are operating in a region of diminishing return. This region, of course, corresponds to the saturation region seen in Fig. 26.

CLOSING COMMENTS

In this article we have discussed windows and alluded to their wide applicability in signal processing. The primary focus was on applications involved with spectrum analysis. We have described the structure of a window in terms of its spectral behavior of its side-lobe levels and main-lobe width. In general, a good window is one that requires a small increase in main-lobe width in order to achieve a specific side-lobe level. System considerations may require different variants of good windows and include windows that exhibit small scallop loss and small-integrated side-lobe levels. We discussed the effect of averaging overlapped, hence correlated, windowed data sets and concluded that the overlap purchased back the processing loss incurred by using a window with larger ENBW. Finally we demonstrated the need for windows in spectral analysis by processing a signal composed of two closely spaced sinewaves of vastly different amplitudes. Other applications of windows such as window design and modulation envelopes follow easily from the basic understanding of how a window affects the windowed spectrum.

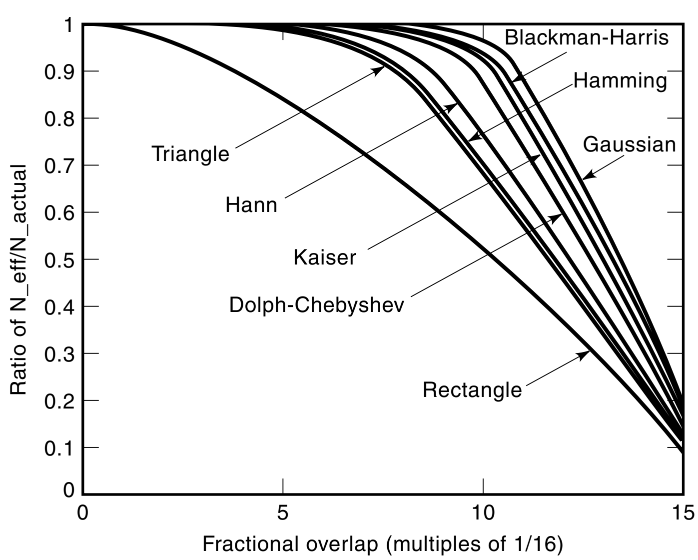

Figure 27. Ratio of N_eff to N_actual as function of overlap.

Reading List

N. C. Gecklili and D. Yarris, Some novel windows and a concise tutorial comparison of window families, *IEEE Trans. Acoust. Speech Signal Process.,* **26**: 501–507, 1978.

F. J. Harris, High resolution spectral analysis with arbitrary spectral centers and adjustable spectral resolution, *J. Comput. Elec. Eng.,* **3**: 171–191, 1976.

F. J. Harris, On the use of windows for harmonic analysis with the discrete Fourier transform, *Proc. IEEE,* **66**: 51–83, 1978.

F. J. Harris, On overlapped fast Fourier transforms, Int. Telemetering Conf. (ITC-78), Los Angeles, 1978, pp. 301–306.

F. J. Harris, The discrete Fourier transform applied to time domain signal processing, *IEEE Commun.,* **20** (3): 13–22, 1982.

J. F. Kaiser and R. W. Schafer, On the use of the Io-Sinh window for spectrum analysis, *IEEE Trans. Acoust., Speech Signal Process.,* **28**: 105, 1980.

A. H. Nuttal, Some windows with very good sidelobe behavior, *IEEE Trans.Acoust., Speech Signal Process.,* **29**: 84–87, 1981.

H. R. Ward, Properties of Dolph-Chebyshev weighting functions, *IEEE Trans. Aerosp. Electron. Syst.,* **9** (5): 785–786, 1973.

P. D. Welch, The use of fast Fourier transform for the estimation of power spectra: A method based on time averaging over short, modified periodograms, *IEEE Trans. Audio Electroacoust.,* **15**: 70–73, 1967.

FRED J. HARRIS
San Diego State University